Mathematical Biosciences and Engineering

http://www.aimspress.com/journal/mbe

MBE, 19(11): 10846–10863.
DOI: 10.3934/mbe.2022507
Received: 25 May 2022
Revised: 26 July 2022
Accepted: 27 July 2022
Published: 29 July 2022

Research article

Isolation in the control of epidemic

Yong Zhou[1,*] **and Minrui Guo**[2]

[1] College of Science, Wuhan University of Science and Technology, Wuhan 430065, China

[2] College of Energy Engineering, Huanghuai University, Zhumadian 463000, China

* **Correspondence:** Email: zhouyongedu@126.com.

Abstract: Among many epidemic prevention measures, isolation is an important method to control the spread of infectious disease. Scholars rarely study the impact of isolation on disease dissemination from a quantitative perspective. In this paper, we introduce an isolation ratio and establish the corresponding model. The basic reproductive number and its biological explanation are given. The stability conditions of the disease-free and endemic equilibria are obtained by analyzing its distribution of characteristic values. It is shown that the isolation ratio has an important influence on the basic reproductive number and the stability conditions. Taking the COVID-19 in Wuhan as an example, isolating more than 68% of the population can control the spread of the epidemic. This method can provide precise epidemic prevention strategies for government departments. Numerical simulations verify the effectiveness of the results.

Keywords: epidemic; isolation ratio; basic reproductive number; stability of equilibrium

1. Introduction

Even if the vaccine is successfully developed and widely vaccinated all over the world, COVID-19 [1–8] still rages around the world. During a pandemic, governments take various measures to slow down the spread of the disease, such as keeping social distance, banning large-scale parties, and even imposing curfews. Strictly controlling the flow of people can combat the epidemic, but it can hurt economic development at the same time. So it is very meaningful to find a suitable isolation ratio which can not only ensure the orderly progress of work and life, but also control the wide spread of the virus. In this paper, we construct a model to analyze the relationship between infected population and social isolation by introducing the isolation ratio.

With the efforts of previous scholars, many typical models have been gradually accumulated, which also reflects that infectious disease model is an important content of research [9–14]. System (1.1) first

proposed by Kermack and McKendrick pioneered the study of infectious diseases [15].

$$\begin{cases} \dot{S} = bN - \beta S I - bS, \\ \dot{I} = \beta S I - \gamma I - (a+b)I, \\ \dot{R} = \gamma I - bR. \end{cases} \tag{1.1}$$

S, R, and I respectively represent susceptible population, recovered population and infected population. The total population N satisfies the equation $N = S+I+R$ without considering the migration population. β is the infected rate, and γ is the recovery rate. The elimination rate of the infected people is $a + b$. SIR model has an assumption that infected patients are immune after rehabilitation. When rehabilitated people are no longer immune to the virus, it means that they are at risk of secondary infection. Then, it becomes SIRS [16, 17] model

$$\begin{cases} \dot{S} = bN - \beta S I - bS + cR, \\ \dot{I} = \beta S I - \gamma I - (a+b)I, \\ \dot{R} = \gamma I - bR, \end{cases} \tag{1.2}$$

where c represents infection rate of convalescent patients. Zhao et al. [17] studied an SIRS model with pulse vaccination and birth pulse. The stability of the infection-free periodic solution and the existence of nontrivial periodic solution which was bifurcated from the infection-free periodic solution were discussed by the Poincaré map and the bifurcation theory. It was obtained when the threshold was reached, a nontrivial periodic solution would appear through supercritical bifurcation.

Since some infectious diseases such as COVID-19 have latent period, asymptomatic infections must be considered. Then SEIR model [18–24] is proposed

$$\begin{cases} \dot{S} = bN - \beta S I - bS, \\ \dot{E} = \beta S I - \gamma E - bE, \\ \dot{I} = \gamma E - (a+b)I, \\ \dot{R} = \gamma I - bR. \end{cases} \tag{1.3}$$

Saikia et al. [18] used SEIR model to predict the epidemic trend in India, and found the existence of peak day, meaning a sudden shift in the mode of disease transmission. In [19], based on the propagation characteristics of COVID-19, SEIR model was improved to SEIQR model and its basic reproductive number was derived. The results showed that the improved model had better predictive power and successfully captured the development process of the COVID-19. When we need to consider that the rehabilitated persons have secondary infection, the system (1.3) becomes SEIRS model [25–27] as follows

$$\begin{cases} \dot{S} = bN - \beta S I - bS + cR, \\ \dot{E} = \beta S I - \gamma E - bE, \\ \dot{I} = \gamma E - (a+b)I, \\ \dot{R} = \gamma I - bR. \end{cases} \tag{1.4}$$

In [25], Britton et al. considered the impact of an infectious disease with escape ability on population growth. Four possible results were obtained in this paper: (1) disease died out quickly, only infecting

few; (2) epidemic took off, but the proportion of infected people was still negligible; (3) infectious disease spread rapidly, and the proportion of infected people had reached a local balance; (4) disease spread widely and rapidly, transforming exponential population growth into exponential decay. Lu et al. [26] proposed a new criterion for determining the global asymptotic stability of nonlinear systems, which was based on the geometric method proposed by Li and Muldowney. Otunuga et al. [27] estimated and analyzed the time-dependent parameters: symptomatic recovery rate, transmission rate, immunity rate and the effective reproduction number for COVID-19 in the United States during the 01/22/2020–02/25/2021 period based on the SEIRS model, where the infected population was classified as the symptomatic infected population and asymptomatic infectious population. It should be noted that the infectious disease model we discussed, whether SEIR model or SEIRS model, does not have the ability of vertical transmission. In other words, the virus cannot be transmitted to the unborn foetus.

In [28], Abdelaziz et al. investigated a discrete-time SEIR epidemic model with constant vaccination and fractional-order, and got its basic reproduction number. They obtained the local and global stability conditions at equilibriums and discussed two types of codimension one bifurcation which were called Neimark-Sacker bifurcation and flip bifurcation. The criterion used was based on the characteristic coefficient equation instead of the properties of the eigenvalues of the Jacobian matrix. Thirthar et al. [29] established an SI_1I_2R model with general recovery functions and saturated incidence of the disease I_1. The local stability and global stability of disease-free equilibrium and endemic equilibrium were given by the basic reproductive number and Lyapunov function. The system studied had neither Saddle-node bifurcation and Transcritical bifurcation near the disease-free equilibrium point under $c_2\beta_2 S_0 < \mu + \epsilon_1 + \epsilon_2$ and $E_0 = 1$. Liu et al. [30] studied the existence and uniqueness of the positive solution in the transmission of two diseases between two groups, which could be called $S_1I_1R_1S_2I_2R_2$ model.

Most works on infectious disease models mainly study the prediction of future trends based on statistical data from different regions. This paper introduces the isolation ratio and establishes the SI_aI_sQR model where S, I_a, I_s, Q and R respectively represent susceptible, asymptomatic, symptomatic, quarantined and recovery classes. We give the basic reproductive number of the model and its biological significance. The stability conditions of the disease-free and endemic equilibria are obtained by analyzing its distribution of characteristic values. The results show that isolation ratio has an important impact on the basic reproductive number and the stability conditions. As p increases, R_0 decreases, and this effect is amplified by square. The simulation results verify the influence of isolation ratio on the system. The rest of this paper is as follows. In Section 2, we establish an SI_aI_sQR model. In Section 3, we obtain the basic reproductive number and give its biological explanation. In Section 4, the stability conditions of the disease-free and endemic equilibria are discussed. In Section 5, we investigate the influence of several important parameters on epidemic spread from numerical simulations. Finally, in Section 6, we summarize and discuss this paper.

2. Modeling

In recent years, in view of the frequent attacks of infectious diseases on humans, experts and scholars have established various models according to different propagation characteristics [31–34]. In this paper, we divide the crowd into five storerooms, which are susceptible class ($S(t)$), asymptomatic in-

fection class ($I_a(t)$), symptomatic infection class ($I_s(t)$), quarantine class ($Q(t)$), and recovery class ($R(t)$), assuming the general population is $N(t) = S(t) + I_a(t) + I_s(t) + Q(t) + R(t)$.

Susceptible class ($S(t)$): It is assumed that the input of the population is a constant (Λ) and the natural mortality of the population is μ. Both symptomatic patients and asymptomatic patients have the ability to infect, and the transmission ability of symptomatic patients is stronger than that of asymptomatic patients ($\alpha_a < \alpha_s$). The proportion of people isolated by the government is p. The contact between susceptible people and infected people is $\alpha_a S(1-p)I_a(1-p) + \alpha_s S(1-p)I_s(1-p)$. There is no vertical transmission of the disease. The change rate of susceptible groups is

$$\dot{S} = \Lambda - \alpha_a(1-p)^2 S I_a - \alpha_s(1-p)^2 S I_s - \mu S.$$

Remark 1 In the process of disease transmission, the infection process has a linear and proportional relationship with $(1-p)^2$, because the isolated objects include infected class and susceptible class. From the perspective of spatial density, if two groups are reduced by the same proportion of p, then the probability of meeting becomes $(1-p)^2$ of the original ones. In the predator-prey model, if the proportion of sheltered prey is q, the probability of predator and prey meeting is $1-q$ of the original ones. It is a linear and proportional relation between the predatory process and $1-q$, because the shelter only acts on the prey [35].

Asymptomatic class ($I_a(t)$): It is assumed that all infected persons will experience a incubation period, and the infected persons in the incubation period will be transformed into symptomatic patients in a fixed proportion of β. The change rate of asymptomatic groups is

$$\dot{I}_a = \alpha_a(1-p)^2 S I_a + \alpha_s(1-p)^2 S I_s - \beta I_a - \mu I_a.$$

Symptomatic class ($I_s(t)$): Symptomatic infected persons will be detected and admitted to hospitals for isolation in proportion to γ. The recovery and mortality rate of infected patients without treatment are δ_1 and $\mu_1 + \mu$. Then, the change rate of symptomatic class is

$$\dot{I}_s = \beta I_a - \gamma I_s - \delta_1 I_s - \mu_1 I_s - \mu I_s.$$

Quarantined class ($Q(t)$): Because of medical treatment, the cure rate of isolated patients will be higher and the mortality rate will be lower than the symptomatic class $\delta_2 > \delta_1$, $\mu_2 < \mu_1$. Differential equation on quarantined class ($Q(t)$) is

$$\dot{Q} = \gamma I_s - \delta_2 Q - \mu_2 Q - \mu Q.$$

Recovery class ($R(t)$): The recovery class comes from symptomatic class in the proportion δ_1 and quarantined class in proportion δ_2. Then we get

$$\dot{R} = \delta_1 I_s + \delta_2 Q - \mu R.$$

Integrating the above five dimensions, we obtain

$$\begin{cases} \dot{S} = \Lambda - \alpha_a(1-p)^2 S I_a - \alpha_s(1-p)^2 S I_s - \mu S, \\ \dot{I}_a = \alpha_a(1-p)^2 S I_a + \alpha_s(1-p)^2 S I_s - \beta I_a - \mu I_a, \\ \dot{I}_s = \beta I_a - \gamma I_s - \delta_1 I_s - \mu_1 I_s - \mu I_s, \\ \dot{Q} = \gamma I_s - \delta_2 Q - \mu_2 Q - \mu Q, \\ \dot{R} = \delta_1 I_s + \delta_2 Q - \mu R. \end{cases} \tag{2.1}$$

The initial conditions of system (2.1) are $S(t_0) = S^0 \geq 0, I_a(t_0) = I_a^0 \geq 0, I_s(t_0) = I_s^0 \geq 0$ $Q(t_0) = Q^0 \geq 0, R(t_0) = R^0 \geq 0$. In order to ensure the biological significance of system (2.1), all solutions must be limited to the positive five dimensional Euclidean space region.

Lemma 2.1 All solutions of system (2.1) with nonnegative initial values keep positive in $\mathbf{R}^5_+$ for all $t > 0$. All solutions of system (2.1) with nonnegative initial values are uniformly bounded in $\mathbf{\Omega} = \{(S, I_a, I_s, Q, R) \in \mathbf{R}^5_+ : 0 \le S, I_a, I_s, Q, R \le \frac{\Lambda}{\mu}\}$.

3. Basic reproductive number

The basic reproductive number is an important reference index for the study of infectious disease model, which represents the number of people infected by each patient during the disease period. The most commonly used method to calculate the basic reproductive number (R_0) is the next-generation matrix [36]. The following is the general process.

Let

$$\frac{dx_i}{dt} = f_i(x) = r_i(x) - h_i(x), i = 1, 2, \cdots, m, \tag{3.1}$$

where $r_i(x)$ is the rate of newly infected individuals in group i, $h_i(x)$ is the transfer rate. Denote $\mathbf{F} = [\frac{\partial r_i}{\partial x_j}(x_0)]$, $\mathbf{V} = [\frac{\partial h_i}{\partial x_j}(x_0)]$, where $x_0 = \{x | x_i = 0, i = 1, 2, \cdots, m\}, 1 \le i, j \le m$. $\mathbf{FV}^{-1}$ is the reproducing matrix. $\rho(\mathbf{FV}^{-1})$ is the spectral radius of the reproducing matrix. R_0 is equal to $\rho(\mathbf{FV}^{-1})$ representing the largest modulus of the eigenvalues of the Jacobian matrixes.

Rewrite system (2.1) to $X = [I_a, I_s, Q, S, R]^T$. The disease-free equilibrium is $x_0 = (I_a(0), I_s(0), Q(0), S(0), R(0)) = (0, 0, 0, \frac{\Lambda}{\mu}, 0)$. According to Eq (3.1),

$$r_i(x) = \begin{bmatrix} \alpha_s(1-p)^2 S I_s + \alpha_a(1-p)^2 S I_a \\ 0 \\ 0 \\ 0 \\ 0 \end{bmatrix},$$

$$h_i(x) = \begin{bmatrix} \beta I_a + \mu I_a \\ -\beta I_a + \gamma I_s + \delta_1 I_s + \mu_1 I_s + \mu I_s \\ -\gamma I_s + \delta_2 Q + \mu_2 Q + \mu Q \\ -\Lambda + \alpha_s(1-p)^2 S I_s + \alpha_a(1-p)^2 S I_a + \mu S \\ -\delta_1 I_s - \delta_2 Q + \mu R \end{bmatrix},$$

$i = 1, 2, 3, 4, 5$. Then, we calculate the Jacobian matrix of $r(x_i)$ and $h(x_i)$ on disease-free equilibrium

$$F(x_0) = \frac{\partial r(x_i)}{\partial x_j}(x_0) = \begin{bmatrix} \alpha_a(1-p)^2\frac{\Lambda}{\mu} & \alpha_s(1-p)^2\frac{\Lambda}{\mu} & 0 & 0 & 0 \\ 0 & 0 & 0 & 0 & 0 \\ 0 & 0 & 0 & 0 & 0 \\ 0 & 0 & 0 & 0 & 0 \\ 0 & 0 & 0 & 0 & 0 \end{bmatrix},$$

$$V(x_0) = \frac{\partial h(x_i)}{\partial x_j}(x_0) = \begin{bmatrix} M_1 & 0 & 0 & 0 & 0 \\ -\beta & M_2 & 0 & 0 & 0 \\ 0 & -\gamma & M_3 & 0 & 0 \\ \alpha_a(1-p)^2\frac{\Lambda}{\mu} & \alpha_s(1-p)^2\frac{\Lambda}{\mu} & 0 & \mu & 0 \\ 0 & -\delta_1 & -\delta_2 & 0 & \mu \end{bmatrix},$$

where $M_1 = \beta + \mu$, $M_2 = \gamma + \delta_1 + \mu_1 + \mu$, $M_3 = \delta_2 + \mu_2 + \mu$, $1 \le i, j \le 5$. Denote

$$F_1 = \begin{bmatrix} \alpha_a(1-p)^2\frac{\Lambda}{\mu} & \alpha_s(1-p)^2\frac{\Lambda}{\mu} \\ 0 & 0 \end{bmatrix},$$

$$V_1 = \begin{bmatrix} \beta + \mu & 0 \\ -\beta & \gamma + \delta_1 + \mu_1 + \mu \end{bmatrix}.$$

We obtain

$$FV^{-1} = F_1V_1^{-1} = \begin{bmatrix} A_1 & A_2 \\ 0 & 0 \end{bmatrix},$$

where

$$A_1 = \alpha_a(1-p)^2\frac{\Lambda}{\mu}\frac{1}{\beta+\mu} + \alpha_s(1-p)^2\frac{\Lambda}{\mu}\frac{\beta}{(\beta+\mu)(\gamma+\delta_1+\mu_1+\mu)},$$

$$A_2 = \alpha_s(1-p)^2\frac{\Lambda}{\mu}\frac{1}{\gamma+\delta_1+\mu_1+\mu}.$$

Hence, the basic reproductive number is

$$R_0 = \rho(FV^{-1}) = R_0^a + R_0^s,$$

where

$$R_0^a = \alpha_a(1-p)^2\frac{\Lambda}{\mu}\frac{1}{\beta+\mu},$$

$$R_0^s = \alpha_s(1-p)^2\frac{\Lambda}{\mu}\frac{\beta}{\beta+\mu}\frac{1}{\gamma+\delta_1+\mu_1+\mu}.$$

Remark 2 $\frac{1}{\beta+\mu}$ and $\frac{1}{\gamma+\delta_1+\mu_1+\mu}$ represent the average removal time of the asymptomatic and symptomatic patients respectively. $\frac{\beta}{\beta+\mu}$ is the ratio of asymptomatic patients to symptomatic patients. R_0^a and R_0^s can be regarded as the number of people infected by each asymptomatic patient and symptomatic patient during the infectious period. As p increases, R_0 decreases, and this effect is amplified by square. This shows that isolation is a very good measure to control the spread of disease. We compare the R_0 of five different models [31, 37–40]. The same parameters of the different basic reproductive numbers have the same effect in their respective models, such as conversion rate and infection rate.

4. Stability of equilibrium point

In this section, we show the local and global stability of the disease-free and endemic equilibria respectively.

4.1. Stability analysis of disease-free equilibrium

In this part, we will discuss the local stability of system (2.1) at the equilibrium point $x_0 = (\frac{\Lambda}{\mu}, 0, 0, 0, 0)$, and we also use Lyapunov function to judge its global stability.

Theorem 1 When $R_0 < 1$, the equilibrium point x_0 of system (2.1) is locally stable; When $R_0 > 1$, it is unstable [36].

Theorem 2 The disease-free equilibrium point is global stable with $R_0 < 1$.

Proof. We construct the Lyapunov function

$$V(t) = (\gamma + \delta_1 + \mu_1 + \mu)I_a(t) + \alpha_s(1-p)^2\frac{\Lambda}{\mu}I_s(t).$$

Obviously, $V(t) \geq 0$.
By direct calculation

$$\begin{aligned}\frac{dV(t)}{dt} &= B_5[\alpha_s(1-p)^2 S I_s + \alpha_a(1-p)^2 S I_a - \beta I_a \\ &- \mu I_a] + \alpha_s(1-p)^2\frac{\Lambda}{\mu}(\beta I_a - \gamma I_s - \delta_1 I_s - \mu_1 I_s - \mu I_s) \\ &= [B_5\alpha_a(1-p)^2 S - (\beta+\mu)B_5 + \alpha_s(1-p)^2\frac{\Lambda}{\mu}\beta]I_a \\ &+ [B_5\alpha_s(1-p)^2 S - \alpha_s(1-p)^2\frac{\Lambda}{\mu}(\gamma + \delta_1 + \mu_1 + \mu)]I_s.\end{aligned}$$

As $S \leq \frac{\Lambda}{\mu}$,

$$\begin{aligned}\frac{dV(t)}{dt} &\leq [B_5\alpha_a(1-p)^2\frac{\Lambda}{\mu} - (\beta+\mu)B_5 + \alpha_s(1-p)^2\frac{\Lambda}{\mu}\beta]I_a \\ &+ [B_5\alpha_s(1-p)^2\frac{\Lambda}{\mu} - \alpha_s(1-p)^2\frac{\Lambda}{\mu}B_5]I_s \\ &= (R_0 - 1)B_5(\beta+\mu)I_a.\end{aligned}$$

When $R_0 < 1$, $\frac{dV_t}{dt} \leq 0$. According to the second Lyapunov method, the disease-free equilibrium point is globally gradually steady.

4.2. Stability of endemic equilibrium

Before discussing the stability of the endemic disease, we consider its existence.

Theorem 3 The positive equilibrium $x^* = (S^*, I_a^*, I_s^*, Q^*, R^*)$ of system (2.1) exists if $R_0 > 1$ is satisfied. When $D_1D_2 > D_3 > 0$ is also satisfied, where
$D_1 = 2\mu + \beta + m + \alpha_s(1-p)^2 I_s^* + \alpha_a(1-p)^2 I_a^* - \alpha_a(1-p)^2 S^*$,
$D_2 = [\beta + \mu - \alpha_a(1-p)^2 S^* + \alpha_s(1-p)^2 I_s^* + \alpha_a(1-p)^2 I_a^*](\mu + c) + \mu c - \beta\alpha_s(1-p)^2 S^*$,
$D_3 = [\beta + \mu - \alpha_a(1-p)^2 S^* + \alpha_s(1-p)^2 I_s^* + \alpha_a(1-p)^2 I_a^*]\mu c - \mu\beta\alpha_s(1-p)^2 S^*$,
the positive equilibrium is locally stable.

Proof. By solving the zero solution of system (2.1), we get $x^* = (S^*, I_a^*, I_s^*, Q^*, R^*)$, where

$$\begin{aligned} S^* &= \frac{(\beta+\mu)B_5}{\alpha_s(1-p)^2\beta + \alpha_a(1-p)^2B_5}, \\ I_a^* &= \frac{\Lambda}{\beta+\mu} - \frac{\mu B_5}{\alpha_s(1-p)^2\beta + \alpha_a(1-p)^2B_5}, \\ I_s^* &= \frac{\beta}{B_5}I_a^*, \\ Q^* &= \frac{\gamma}{\delta_2+\mu_2+\mu}I_s^*, \\ R^* &= \frac{\delta_1}{\mu}I_s^* + \frac{\delta_2}{\mu}Q^*. \end{aligned}$$

We just need to judge the negative and positive of I_a^*. By direct calculation,

$$I_a^* = \frac{C_1 - C_2}{(\beta+\mu)(\alpha_s(1-p)^2\beta + \alpha_a(1-p)^2B_5)},$$

where, $C_1 = \Lambda(\alpha_s\beta + \alpha_a B_5, C_2 = (\beta+\mu)\mu B_5$. Note that, $C_1 - C_2 > 0$, i.e., $\frac{C_1}{C_2} - 1 > 0$. Then,

$$\begin{aligned} \frac{C_1}{C_2} &= \frac{\Lambda(\alpha_s(1-p)^2\beta + \alpha_a(1-p)^2B_5}{(\beta+\mu)\mu B_5} \\ &= \frac{\Lambda\alpha_s(1-p)^2\beta}{(\beta+\mu)\mu B_5} + \frac{\Lambda\alpha_a(1-p)^2}{(\beta+\mu)\mu} \\ &= R_0. \end{aligned}$$

So when $R_0 > 1$, $I_a^* > 0$. The positive equilibrium of system (2.1) exists. The Jacobian matrix of system (2.1) at the positive equilibrium point is

$$J_{(x^*)} = \begin{bmatrix} E_1 & E_2 & E_3 & 0 & 0 \\ E_4 & E_5 & E_6 & 0 & 0 \\ 0 & \beta & -B_5 & 0 & 0 \\ 0 & 0 & \gamma & -B_6 & 0 \\ 0 & 0 & \delta_1 & \delta_2 & -\mu \end{bmatrix},$$

where $E_1 = -\alpha_s(1-p)^2I_s^* - \alpha_a(1-p)^2I_a^* - \mu, E_2 = -\alpha_a(1-p)^2S^*, E_3 = -\alpha_s(1-p)^2S^*, E_4 = \alpha_s(1-p)^2I_s^* + \alpha_a(1-p)^2I_a^*, E_5 = \alpha_a(1-p)^2S^* - \beta - \mu, E_6 = \alpha_s(1-p)^2S^*$.

Then, we get

$$|\lambda E - J_{(x^*)}| = (\lambda+\mu)(\lambda+\delta_2+\mu_2+\mu)(\lambda^3 + D_1\lambda^2 + D_2\lambda + D_3),$$

where $D_1 = 2\mu + \beta + m + \alpha_s(1-p)^2I_s^* + \alpha_a(1-p)^2I_a^* - \alpha_a(1-p)^2S^*, D_2 = [\beta + \mu - \alpha_a(1-p)^2S^* + \alpha_s(1-p)^2I_s^* + \alpha_a(1-p)^2I_a^*](\mu + c) + \mu c - \beta\alpha_s(1-p)^2S^*, D_3 = [\beta + \mu - \alpha_a(1-p)^2S^* + \alpha_s(1-p)^2I_s^* + \alpha_a(1-p)^2I_a^*]\mu c - \mu\beta\alpha_s(1-p)^2S^*$.

According to the Routh-Hurwitz theorem,

$$\Delta_1 = D_1 > 0, \qquad \Delta_2 = \begin{vmatrix} D_1 & 1 \\ D_3 & D_2 \end{vmatrix} > 0, \Delta_3 = \begin{vmatrix} D_1 & 1 & 0 \\ D_3 & D_2 & D_1 \\ 0 & 0 & D_3 \end{vmatrix} > 0.$$

We obtain $D_1 > 0, D_1D_2 > D_3 > 0$.

Table 1. Parameters estimation of Model (5.1).

Parameters	Definitions	Values	Source
μ	Mortality	$1.6 \times 10^{-5} day^{-1}$	[41]
N	Total population	1.11×10^7	[41]
α_a	Transmission rate of asymptomatic infection	$2.1 \times 10^{-8} day^{-1}$	[39]
α_s	Transmission rate of symptomatic infection	$1.9 \times 10^{-7} day^{-1}$	[39]
γ	Detection rate	$0.13 day^{-1}$	[39]
σ^{-1}	Mean latent period	$2 days$	[42]
τ^{-1}	Mean infectious period	$3 days$	[42]
κ^{-1}	Mean duration from loss infectiousness to death	$8 days$	[42]

5. Numerical simulations and discussions

This section is divided into four parts. Subsection 5.1 mainly discusses the influence of the incubation period from asymptomatic to symptomatic patients. Subsection 5.2 studies the impact of the infectious period on disease dissemination. In Subsection 5.3, we focus on the relationship between isolation ratio and epidemic spread. In this subsection, we obtain the isolation ratio to control the spread of the epidemic. In Subsection 5.4, the simulations show the disease-free and endemic equilibria of system 2.1 are stable with certain conditions.

5.1. Influence of incubation period

This section mainly discusses the influence of the incubation period on disease dissemination. We simulate the outbreak of the COVID-19 in Wuhan [39, 43–46]. To simplify parameter estimation, we make $\sigma = \beta + \mu, \tau = \gamma + \delta_1 + \mu_1 + \mu, \kappa = \delta_2 + \mu_2 + \mu$. So system (2.1) can be simplified as

$$\begin{cases} \dot{S} = \Lambda - \alpha_a(1-p)^2 S I_a - \alpha_s(1-p)^2 S I_s - \mu S, \\ \dot{I}_a = \alpha_a(1-p)^2 S I_a + \alpha_s(1-p)^2 S I_s - \sigma I_a, \\ \dot{I}_s = \sigma I_a - \tau I_s, \\ \dot{Q} = \tau I_s - \kappa Q. \end{cases} \tag{5.1}$$

Relevant parameters are shown in Table 1. The initial value of system (5.1) is $(S(0), I_a(0), I_s(0), Q(0)) = (1.11 \times 10^7, 105, 28, 1)$ [39].

As σ is the conversion rate from asymptomatic to symptomatic infections, σ^{-1} can be seen the incubation period from asymptomatic to symptomatic infections. The incubation period of COVID-19 is 2–14 days [47]. We study the spread of COVID-19 by changing the incubation period without considering isolation. When the value range of σ^{-1} is 2 to 14, the reproductive number of system (5.1) is greater than 1, and the COVID-19 will spread. Figure 1a shows the change of S when $\sigma = 1/2, 1/6, 1/10, 1/14$. It can be seen that all susceptible persons will be infected if nothing is done. We can also see from Figure 1a that the higher the conversion rate, the faster the dissemination speed. Figure 1b shows the change of I_a when $\sigma = 1/2, 1/6, 1/10, 1/14$. It can be seen that the longer the incubation period, the greater the peak value of asymptomatic infections. When the incubation period

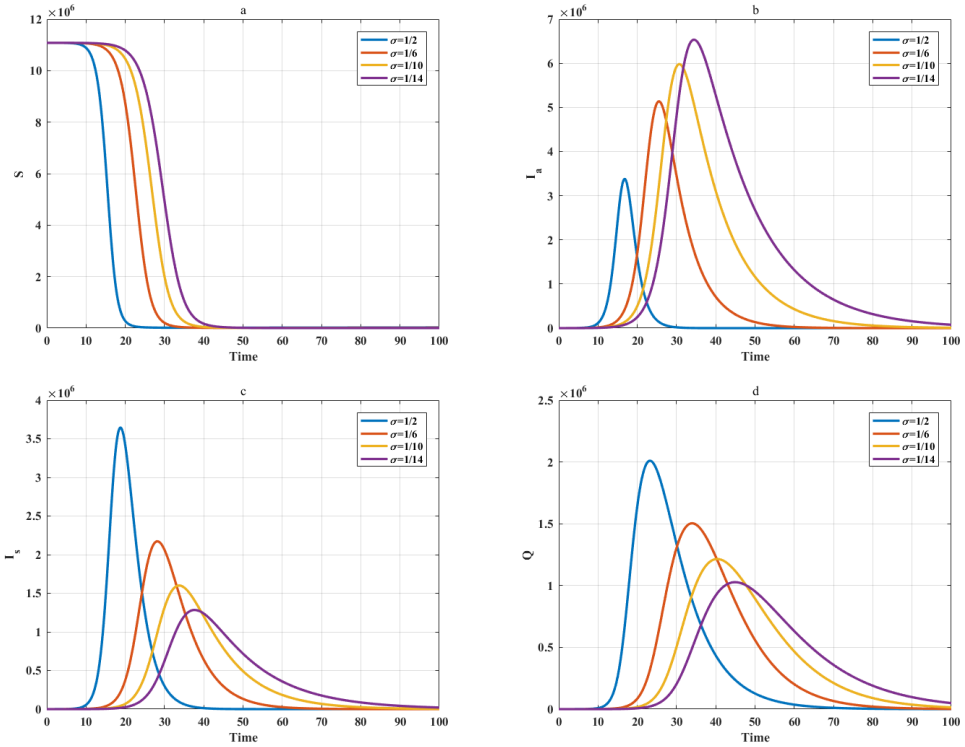

Figure 1. Sequence diagrams for S, I_a, I_s, Q with $\sigma = 1/2, 1/6, 1/10, 1/14$.

is shorter, the peak infection will come faster for asymptomatic infections. Figure 1c shows the change of I_s when $\sigma = 1/2, 1/6, 1/10, 1/14$. Contrary to asymptomatic infections, the shorter the incubation period, the greater the peak value for symptomatic infections. When the incubation period is shorter, the peak infection will also come faster for symptomatic infections. Figure 1d shows the change of Q when $\sigma = 1/2, 1/6, 1/10, 1/14$. When the incubation period is longer, the peak of infections will be lower and arrive later. To sum up, the longer the incubation period, the slower the disease spreads and the greater the peak. One reason why COVID-19 can spread across the world is largely due to its long incubation period.

5.2. Influence of infectious period

This section studies the impact of the infectious period on disease dissemination without isolation. τ is the elimination rate of symptomatic population, then τ^{-1} can represent its infectious period. The parameters follow the subsection 5.1. When τ is equal to 1/2, 1/3, 1/4 and 1/5, the reproductive numbers are greater than 1, and the COVID-19 will spread. Figure 2a shows the larger τ is, the slower S decreases. This means that the longer the infectious period, the faster the transmission speed. Figure 2b shows the longer the infectious period, the higher the asymptomatic infections. The peak will come earlier for the smaller elimination rate. The curves of symptomatic infections are similar to that of asymptomatic infections, which is shown in Figure 2c. However, there is little difference in the time of peak for symptomatic infections under different τ. Figure 2d is similar to Figure 2c. Its peak is lower and later. It is concluded that the longer the infectious period, the more infected people, and the faster the dissemination speed.

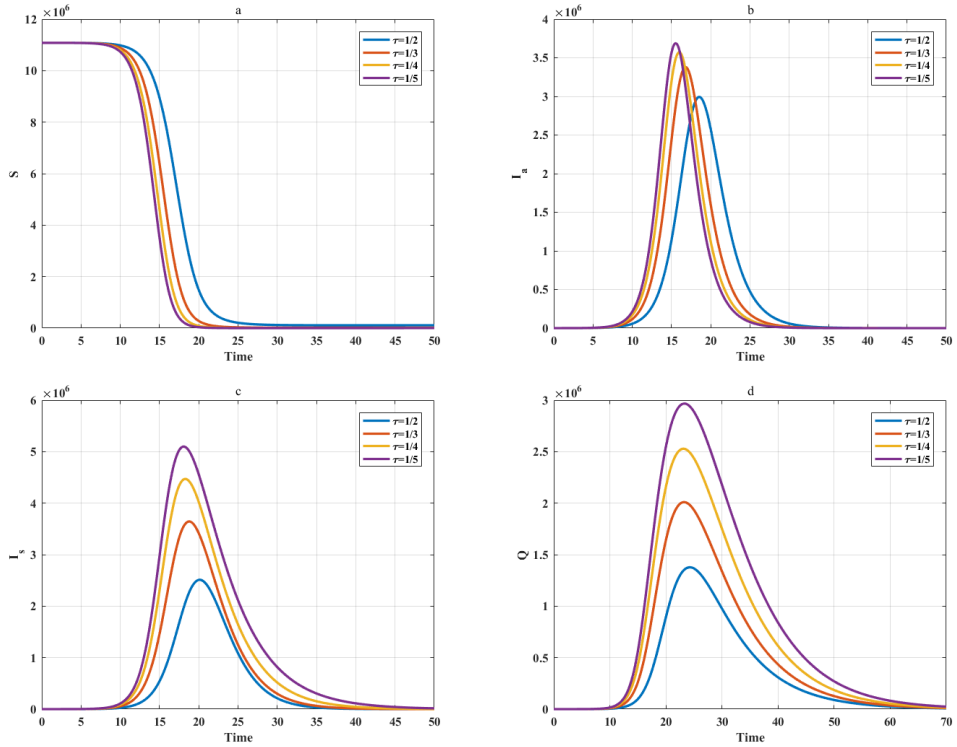

Figure 2. Sequence diagrams for S, I_a, I_s, Q with $\tau = 1/2, 1/3, 1/4, 1/5$

5.3. Influence of isolation ratio

This section studies the impact of different isolation ratios on disease dissemination when the incubation periods from asymptomatic to symptomatic infections are 1/2, 1/7 and 1/14. Except for σ, the values of other parameters are the same as those in Subsection 5.1. Figures 3–5 are sequence diagrams for S, I_a, I_s, Q of $\sigma = 1/2, 1/7$, and $1/14$. We study the spread of the COVID-19 by changing the isolation ratio.

Figure 3 shows the curves of the disease dissemination with the isolation ratio from 0 to 70% during the 2-day incubation period. When $p < 0.5$, the number of infections is millions. When $0.5 < p < 0.6$, the number drops to six figures. When the isolation ratio exceeds 60%, the number of infected people will not exceed tens of thousands. When the isolation ratio exceeds 62%, the epidemic will not spread. Therefore, in view of the outbreak of COVID-19 in Wuhan, theoretically controlling the flow of more than 62% of people can prevent the wide spread.

Figure 4 shows the curves of the disease dissemination with the isolation ratio from 0 to 70% during the 7-day incubation period. When $0 < p < 0.5$, the number of infections is millions. When $0.55 < p < 0.62$, the number drops to six figures. When the isolation ratio exceeds 62%, the number of infected people will not exceed tens of thousands. When the isolation ratio exceeds 65%, the epidemic will not spread.

Figure 5 shows the curves of the disease dissemination with the isolation ratio from 0 to 75% during the 14-day incubation period. When $0 < p < 0.6$, the number of infections is millions. When $0.6 < p < 0.65$, the number drops to six figures. When the isolation ratio exceeds 65%, the number of

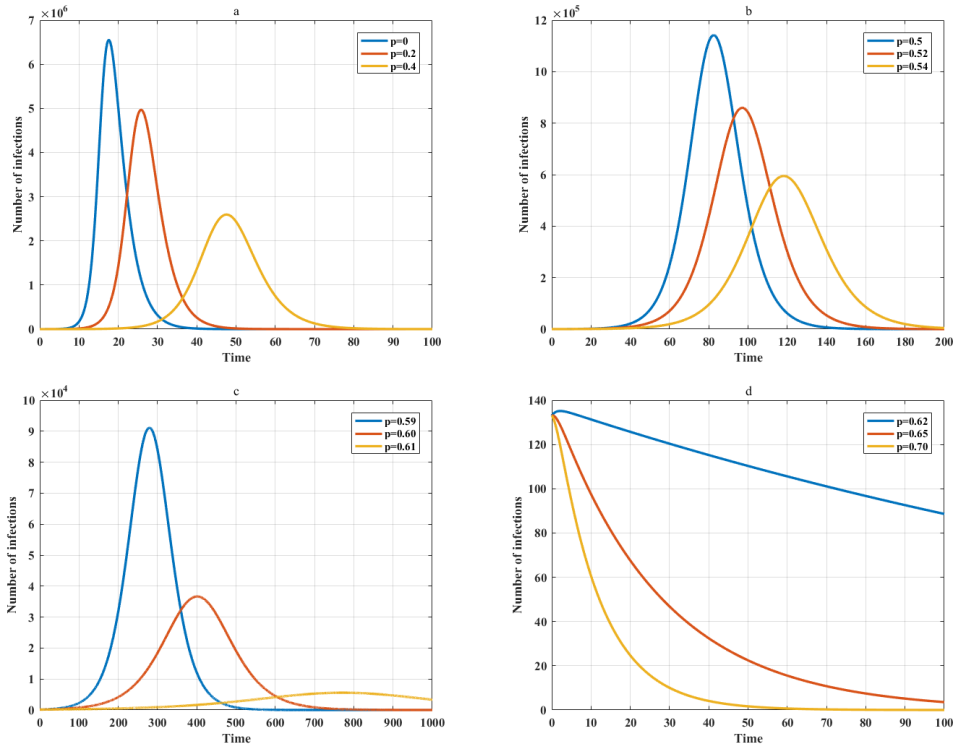

Figure 3. Sequence diagrams for S, I_a, I_s, Q with 2-day incubation period.

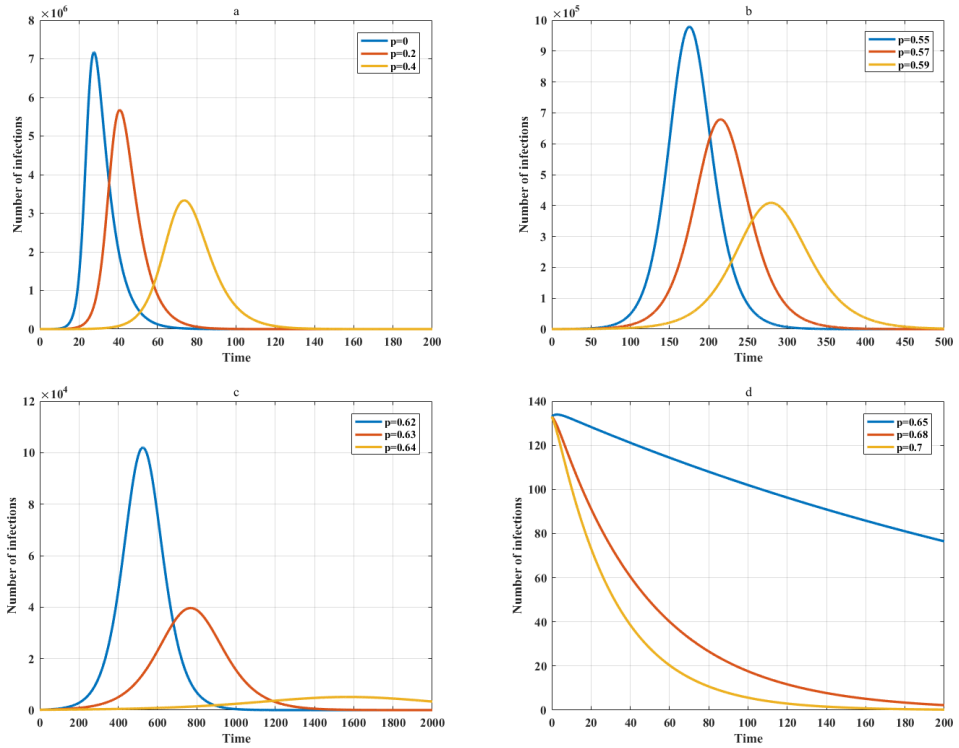

Figure 4. Sequence diagrams for S, I_a, I_s, Q with 7-day incubation period.

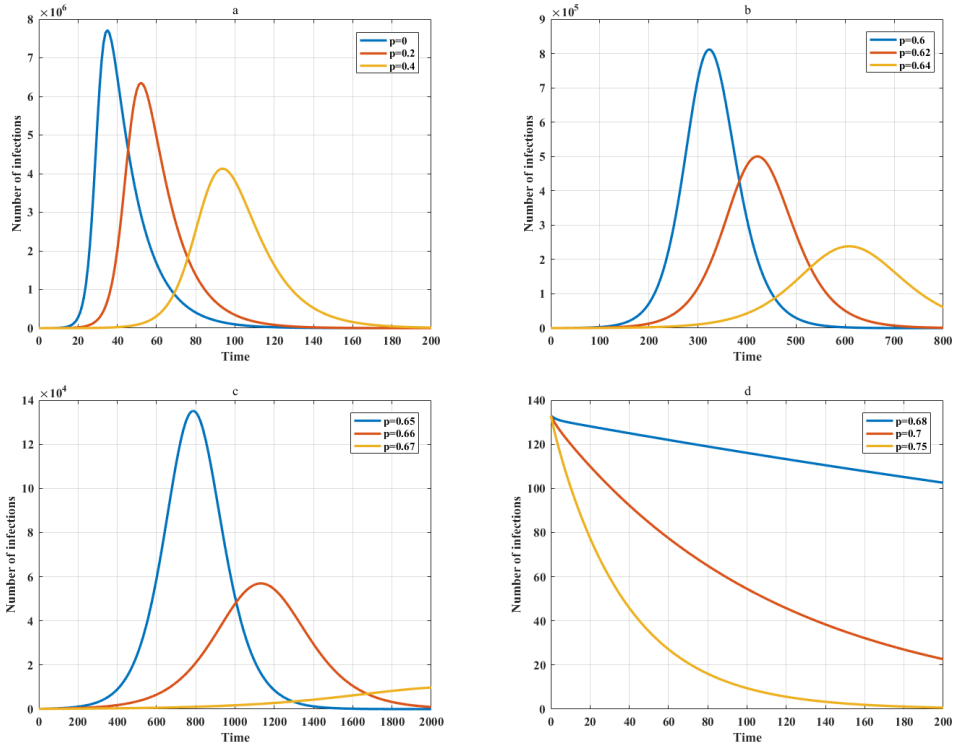

Figure 5. Sequence diagrams for S, I_a, I_s, Q with 14-day incubation period.

infected people will not exceed tens of thousands. When the isolation ratio exceeds 68%, the epidemic will not spread.

Through the above analysis, in order to stop the spread of COVID-19 in Wuhan, the isolation ratio should exceed 68%. Comparing Figures 3–5, we can find when the incubation period increases, the isolation ratio required to control the spread will increase. An important reason why COVID-19 is widely spread around the world is that its incubation period is very long.

5.4. Simulations of disease-free and endemic equilibria

This subsection presents the stability of disease-free and endemic equilibria through simulation. In order to verify that the disease-free equilibrium is globally stable, the parameters of system (2.1) meet $R_0 < 1$. The initial value is $(S(0), I_a(0), I_s(0), Q(0), R(0)) = (800000, 700, 400, 300, 200)$. Figure 6a proves the number of susceptible population is constant by changing the initial value of S. Figure 6b, c and d show the numbers of asymptomatic, symptomatic and quarantined infections tend to 0 under different initial values. Therefor the disease-free equilibrium of system (2.1) is stable when $R_0 < 1$.

System (2.1) has an endemic equilibrium when the parameters conform to $R_0 > 1$. Select the initial value as $(S(0), I_a(0), I_s(0), Q(0), R(0)) = (800000, 700, 400, 300, 200)$. When the initial value of S is changed, different curves eventually tend to the same positive value which can be seen in Figure 7a. Applying the same method to I_a, I_s, Q, we get Figure 7b, c and d. Therefor system (2.1) has an endemic equilibrium with $R_0 > 1$, and it is stable.

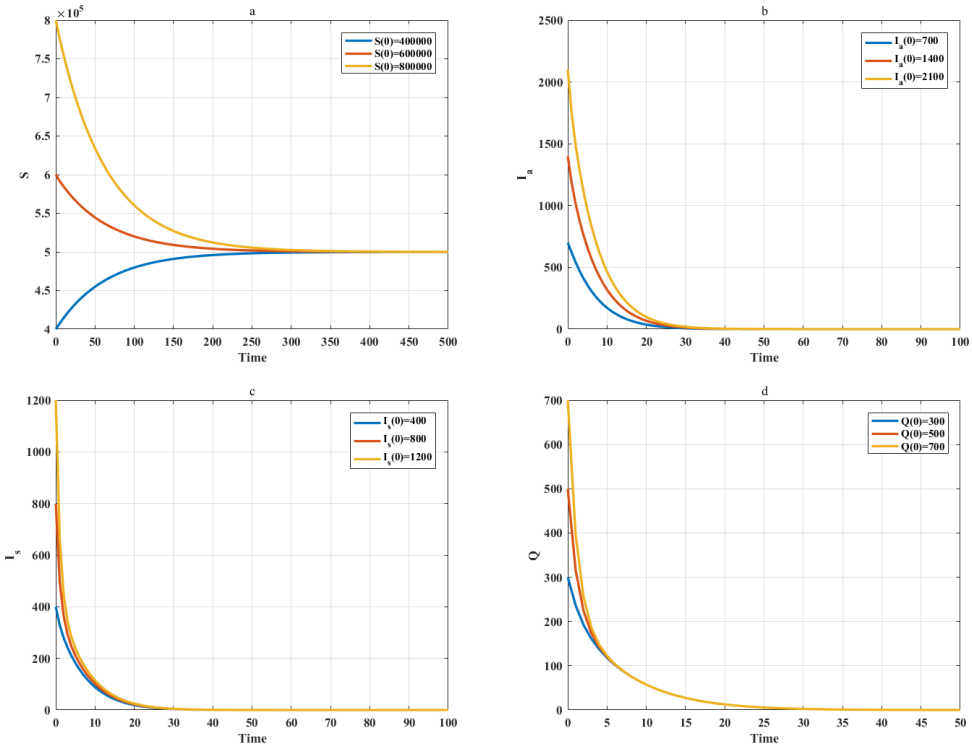

Figure 6. Sequence diagrams with $R_0 = 0.76$.

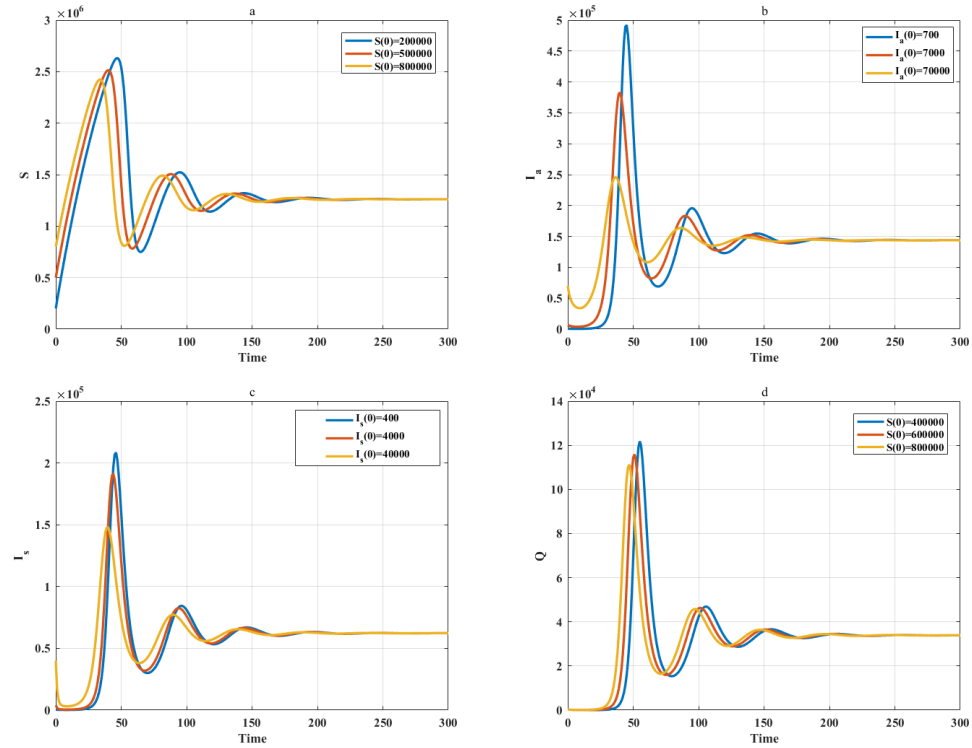

Figure 7. Sequence diagrams with $R_0 = 2.28$.

6. Conclusions

In this paper, we introduce the isolation ratio to quantify the impact of isolation on diseases dissemination. The basic reproductive number solved by the next-generation matrix can be divided into two parts, which are contributed by asymptomatic and symptomatic infections respectively. We obtain the effects of conversion rate from asymptomatic to symptomatic infections, mortality rate of infections and isolation ratio on disease dissemination. Through the stability analysis, we get the local and global stability conditions for the disease-free and endemic equilibria of the system. When $R_0 < 1$, the disease-free equilibrium is globally asymptotically stable; When $R_0 > 1$, the disease-free equilibrium is not stable. When $R_0 < 1$, the positive equilibrium does not exist; When $R_0 > 1$, the positive equilibrium exists and is stable. Taking the outbreak of COVID-19 in Wuhan as an example, when the proportion of the isolated population exceeds 68%, the epidemic will not be spread. Therefore, we can formulate different proportions of isolated population according to different regions. This not only ensures the epidemic will not spread on a large scale, but also does not stop the economic activities.

Acknowledgments

This work was supported by the Science and Technology Research Project of Henan Province (222102240108).

Conflict of interest

The authors declare there is no conflicts of interest.

Data availability statements

The datasets analysed during the current study are available from the corresponding author on reasonable request.

References

1. H. Wang, Z. Wang, Y. Dong, R. Chang, C. Xu, X. Yu, et al., Phase-adjusted estimation of the number of coronavirus disease 2019 cases in wuhan, china, *Cell Discov.*, **6** (2020), 1–8. https://doi.org/10.1038/s41421-020-0148-0
2. D. Wang, M. Zhou, X. Nie, W. Qiu, M. Yang, X. Wang, et al., Epidemiological characteristics and transmission model of corona virus disease 2019 in china, *J. Infect.*, **80** (2020), e25–e27. https://doi.org/10.1016/j.jinf.2020.03.008
3. F. S. Dawood, P. Ricks, G. J. Njie, M. Daugherty, W. Davis, J. A. Fuller, et al., Observations of the global epidemiology of covid-19 from the prepandemic period using web-based surveillance: A cross-sectional analysis, *Lancet Infect. Dis.*, **20** (2020), 1255–1262. https://doi.org/10.1016/S1473-3099(20)30581-8

4. C. Jiang, X. Li, C. Ge, Y. Ding, T. Zhang, S. Cao, et al., Molecular detection of sars-cov-2 being challenged by virus variation and asymptomatic infection, *J. Pharm. Anal.*, **11** (2021), 257–264. https://doi.org/10.1016/j.jpha.2021.03.006
5. F. A. Engelbrecht, R. J. Scholes, Test for covid-19 seasonality and the risk of second waves, *One Health*, **12** (2021), 100202.
6. M. Yao, H. Wang, A potential treatment for covid-19 based on modal characteristics and dynamic responses analysis of 2019-ncov, *Nonlinear Dyn.*, **106** (2021), 1425–1432. https://doi.org/10.1007/s11071-020-06019-1
7. P. Das, R. K. Upadhyay, A. K. Misra, F. A. Rihan, P. Das, D. Ghosh, Mathematical model of covid-19 with comorbidity and controlling using non-pharmaceutical interventions and vaccination, *Nonlinear Dyn.*, **106** (2021), 1213–1227. https://doi.org/10.1007/s11071-021-06517-w
8. K. Shah, Z. A. Khan, A. Ali, R. Amin, H. Khan, A. Khan, Haar wavelet collocation approach for the solution of fractional order covid-19 model using caputo derivative, *Alex. Eng. J.*, **59** (2020), 3221–3231. https://doi.org/10.1016/j.aej.2020.08.028
9. C. Han, Y. Liu, J. Tang, Y. Zhu, C. Jaeger, S. Yang, Lessons from the mainland of China's epidemic experience in the first phase about the growth rules of infected and recovered cases of covid-19 worldwide, *Int. J. Disaster Risk Sci.*, **11** (2020), 497–507. https://doi.org/10.1007/s13753-020-00294-7
10. J. T. Machado, J. Ma, Nonlinear dynamics of covid-19 pandemic: modeling, control, and future perspectives, *Nonlinear Dyn.*, **101** (2020), 1525–1526. https://doi.org/10.1007/s11071-020-05919-6
11. S. He, Y. Peng, K. Sun, Seir modeling of the covid-19 and its dynamics, *Nonlinear Dyn.*, **101** (2020), 1667–1680. https://doi.org/10.1007/s11071-020-05743-y
12. G. Stewart, K. van Heusden, G. A. Dumont, How control theory can help us control covid-19, *IEEE Spectrum*, **57** (2020), 22–29. https://doi.org/10.1109/MSPEC.2020.9099929
13. D. Fanelli, F. Piazza, Analysis and forecast of covid-19 spreading in china, italy and france, *Chaos Solitons Fract.*, **134** (2020), 109761.
14. R. Li, S. Pei, B. Chen, Y. Song, T. Zhang, W. Yang et al., Substantial undocumented infection facilitates the rapid dissemination of novel coronavirus (sars-cov-2), *Science*, **368** (2020), 489–493.
15. W. O. Kermack, A. G. McKendrick, Contributions to the mathematical theory of epidemics. ii.—the problem of endemicity, *Bull. Math. Biol.*, **138** (1932), 55–83.
16. C. Zheng, Complex network propagation effect based on sirs model and research on the necessity of smart city credit system construction, *Alex. Eng. J.*, **61** (2022), 403–418. https://doi.org/10.1016/j.aej.2021.06.004
17. Z. Zhao, L. Pang, Y. Chen, Nonsynchronous bifurcation of sirs epidemic model with birth pulse and pulse vaccination, *Nonlinear Dyn.*, **79** (2015), 2371–2383. https://doi.org/10.1007/s11071-014-1818-y
18. D. Saikia, K. Bora, M. P. Bora, Covid-19 outbreak in india: An seir model-based analysis, *Nonlinear Dyn.*,**104** (2021), 4727–4751.

19. C. Xu, Y. Yu, Y. Chen, Z. Lu, Forecast analysis of the epidemics trend of covid-19 in the usa by a generalized fractional-order seir model, *Nonlinear Dyn.*, **101** (2020), 1621–1634. https://doi.org/10.1007/s11071-020-05946-3
20. R. K. Upadhyay, A. K. Pal, S. Kumari, P. Roy, Dynamics of an seir epidemic model with nonlinear incidence and treatment rates, *Nonlinear Dyn.*, **96** (2019), 2351–2368. https://doi.org/10.1007/s11071-019-04926-6
21. P. Yarsky, Using a genetic algorithm to fit parameters of a covid-19 seir model for us states, *Math. Comput. Simulat.*, **185** (2021), 687–695. https://doi.org/10.1016/j.matcom.2021.01.022
22. N. ben Khedher, L. Kolsi, H. Alsaif, A multi-stage seir model to predict the potential of a new covid-19 wave in ksa after lifting all travel restrictions, *Alex. Eng. J.*, **60** (2021), 3965–3974. https://doi.org/10.1016/j.aej.2021.02.058
23. N. Piovella, Analytical solution of seir model describing the free spread of the covid-19 pandemic, *Chaos Solitons Fract.*, **140** (2020), 110243.
24. S. J. Weinstein, M. S. Holland, K. E. Rogers, N. S. Barlow, Analytic solution of the seir epidemic model via asymptotic approximant, *Physica D.*, **411** (2020), 132633–132633. https://doi.org/10.1016/j.physd.2020.132633
25. T. Britton, D. Ouédraogo, Seirs epidemics with disease fatalities in growing populations., *Math. Biosci.*, **296** (2018), 45–59. https://doi.org/10.1016/j.mbs.2017.11.006
26. G. Lu, Z. Lu, Global asymptotic stability for the seirs models with varying total population size., *Math. Biosci.*, **296** (2018), 17–25. https://doi.org/10.1016/j.mbs.2017.11.010
27. O. M. Otunuga, Estimation of epidemiological parameters for covid-19 cases using a stochastic seirs epidemic model with vital dynamics, *Result. Phys.*, **28** (2021), 104664.
28. M. A. Abdelaziz, A. I. Ismail, F. A. Abdullah, M. H. Mohd, Codimension one and two bifurcations of a discrete-time fractional-order seir measles epidemic model with constant vaccination, *Chaos Solitons Fract.*, **140** (2020), 110104.
29. A. A. Thirthar, R. K. Naji, F. Bozkurt, A. Yousef, Modeling and analysis of an si1i2r epidemic model with nonlinear incidence and general recovery functions of i1, *Chaos Solitons Fract.*, **145** (2021), 110746.
30. L. Liu, D. Jiang, T. Hayat, Dynamics of an sir epidemic model with varying population sizes and regime switching in a two patch setting, *Phys. A.*, **574** (2021), 125992.
31. S. S. Nadim, I. Ghosh, J. Chattopadhyay, Short-term predictions and prevention strategies for covid-19: a model-based study, *Appl. Math. Comput.*, **404** (2021), 126251.
32. S. Khajanchi, K. Sarkar, Forecasting the daily and cumulative number of cases for the covid-19 pandemic in india, *Chaos*, **30** (2020), 071101.
33. D. K. Das, A. Khatua, T. K. Kar, S. Jana, The effectiveness of contact tracing in mitigating covid-19 outbreak: A model-based analysis in the context of india, *Appl. Math. Comput.*, **404** (2021), 126207.
34. Y. Liu, K. Lillepold, J. C. Semenza, Y. Tozan, M. B. Quam, J. Rocklöv, Reviewing estimates of the basic reproduction number for dengue, zika and chikungunya across global climate zones, *Environ. Res.*, **182** (2020), 109114.

35. Y. Zhou, W. Sun, Y. Song, Z. Zheng, J. Lu, S. Chen, Hopf bifurcation analysis of a predator–prey model with holling-ii type functional response and a prey refuge, *Nonlinear Dyn.*, **97** (2019), 1439–1450. https://doi.org/10.1007/s11071-019-05063-w

36. P. Van den Driessche, J. Watmough, Reproduction numbers and sub-threshold endemic equilibria for compartmental models of disease transmission, *Math Biosci.* **180** (2002), 29–48. https://doi.org/10.1016/S0025-5564(02)00108-6

37. M. Samsuzzoha, M. Singh, D. Lucy, Uncertainty and sensitivity analysis of the basic reproduction number of a vaccinated epidemic model of influenza, *Appl. Math. Model.*, **37** (2013), 903–915. https://doi.org/10.1016/j.apm.2012.03.029

38. S. Tchoumi, M. Diagne, H. Rwezaura, J. Tchuenche, Malaria and covid-19 co-dynamics: A mathematical model and optimal control, *Appl. Math. Model.*, **99** (2021), 294–327. https://doi.org/10.1016/j.apm.2021.06.016

39. B. Tang, X. Wang, Q. Li, N. L. Bragazzi, S. Tang, Y. Xiao, et al., Estimation of the transmission risk of the 2019-ncov and its implication for public health interventions, *J. Clin. Med.*, **9** (2020), 462.

40. G. Rohith, K. Devika, Dynamics and control of covid-19 pandemic with nonlinear incidence rates, *Nonlinear Dyn.*, **101** (2020), 2013–2026. https://doi.org/10.1007/s11071-020-05774-5

41. Wuhan Municipal Bureau of Statistics. Available from: http://tjj.wuhan.gov.cn.

42. G. Fan, H. Song, S. Yip, T. Zhang, D. He, Impact of low vaccine coverage on the resurgence of covid-19 in central and eastern europe, *One Health*, **14** (2022), 100402. https://doi.org/10.1016/j.onehlt.2022.100402

43. K. Adhikari, R. Gautam, A. Pokharel, K. N. Uprety, N. K. Vaidya, Transmission dynamics of covid-19 in nepal: Mathematical model uncovering effective controls, *J. Theor. Biol.*, **521** (2021), 110680.

44. A. Ali, F. S. Alshammari, S. Islam, M. A. Khan, S. Ullah, Modeling and analysis of the dynamics of novel coronavirus (covid-19) with caputo fractional derivative, *Results Phys.*, **20** (2021), 103669.

45. A. B. Gumel, E. A. Iboi, C. N. Ngonghala, E. H. Elbasha, A primer on using mathematics to understand covid-19 dynamics: Modeling, analysis and simulations, *Infect. Dis. Model.*, **6** (2021), 148–168.

46. A. M. Salman, I. Ahmed, M. H. Mohd, M. S. Jamiluddin, M. A. Dheyab, Scenario analysis of covid-19 transmission dynamics in malaysia with the possibility of reinfection and limited medical resources scenarios, *Comput. Biol. Med.*, **133** (2021), 104372.

47. Q. Fan, W. Zhang, B. Li, D. J. Li, J. Zhang, F. Zhao, Association between abo blood group system and covid-19 susceptibility in wuhan, *Front. Cell. Infect. Microbiol.*, **10** (2020), 404. https://doi.org/10.3389/fcimb.2020.00404

AIMS Press